Suplemento de la Revista Mexicana de Física **3** 020723 (2022) 1–5

Phenomenological studies in the 2HDM and SM using Madgraph 5

S. L. Sicairos Páez and R. J. Hernández-Pinto

Facultad de Ciencias Físico-Matemáticas, Universidad Autónoma de Sinaloa, Ciudad Universitaria, CP 80000 Culiacán, México.

Received 21 January 2022; accepted 2 May 2022

The phenomenological analysis of an extension of the Standard Model is analyzed in this manuscript. The Two Higgs Doublet Model is a simple way to incorporate a second extra doublet to the Standard Model to reduce the tension between experimental measurements and theoretical predictions. This model presents a large phenomenological signal which could guide the search for new physics at hadron colliders. In particular, we study the transverse momentum, the rapidity and the angular distributions of the jets in the $pp \to jjh$ channel within the Standard Model and the Two Higgs Doublet Model in the LHC and FCC environment by means of Monte Carlo simulations made in MadGraph 5.

Keywords: Quantum chromodynamics; models beyond the standard model; collider physics.

DOI: https://doi.org/10.31349/SuplRevMexFis.3.020723

1. Introduction

The physics at hadron colliders is taking giant steps through the design, construction and technological developments in order to understand the behavior of the most elementary particles. All of them would allow us to reach the precision frontier, where experimental measurements shall be contrasted with precise theoretical predictions. In this spirit, it is imperative to advance together, the experimental and the theoretical aspects, to decipher the dynamics of elementary particles.

The Standard Model (SM) of elementary particles has proven, with great success, its predictive power in the determination of observables at the Large Hadron Collider (LHC). Its breakthrough came in 2012 with the announcement of the discovery of the only scalar particle in the SM, the Higgs boson [1, 2]. However, recent studies at the Fermilab laboratory have put the SM under stress by comparing the measurement of the anomalous magnetic moment of the muon [3]. This result, in conjunction with other results [4], leads researchers to continue to argue that the SM cannot be the end of the road in particle physics and, in addition, to present the SM as an effective model of a larger theory [5]. Furthermore, the non-perturbative regime could also hide physics beyond SM. Understanding the internal dynamics of hadrons requires to explore novel ideas and techniques [6–8], in order to access to the interactions of the fundamental constituents of matter and discover new phenomena.

One of the most attractive alternatives to the SM, without any gauge extension, is to increase the number of scalar fields in the model. Among several options, one of the most favored models to tackle several issues of the SM is the Two Higgs Doublet Model (2HDM). In this document, we study the phenomenological aspects of this model in the environment of the LHC and at the Future Circular Collider (FCC) [9–12]. This manuscript is divided as follows: in Sec. 2 the theoretical description of the 2HDM is discussed; in Sec. 3, the process under consideration and the kinematical cuts implemented for the LHC and the FCC are presented; in addition, the results of the Monte Carlo simulations in MadGraph 5 are presented; and in Sec. 4 we present our conclusions and perspectives of this analysis.

2. Two Higgs doublet model

The fundamental description of nature is well understood through the Standard Model. Even if the SM has explained and predicted many experimental results, it still has unsolved questions, mainly driven by experimental results, such as: neutrino masses [14, 15], the asymmetry between matter and antimatter [13], the origin of dark matter [16–22] and dark energy [23, 24], etc. In order to solve this puzzle, there are several groups devoted to build models beyond the SM, such as the 2HDM [25], one of the simplest models beyond the SM. In this extension, we obtain a different and a more rich phenomenology with respect to the SM predictions. From the theoretical point of view, it contains new scalar states such as: two charged Higgs Bosons ($H^{\pm}$), a CP odd pseudoscalar (A), and two Higgs-like bosons, the light Higgs (h), and the heavy Higgs (H). The light Higgs is associated with the SM Higgs boson with a mass of $m_h = 125.25$ GeV [26]. Both, the light and heavy Higgs acquire a vacuum expectation value and they are both responsible for the masses of the SM particles. The potential of the 2HDM type II (where FCNC are ignored) is given by,

$$\begin{aligned} V = {} & \mu_1 \Phi_1^\dagger \Phi_1 + \mu_2 \Phi_2^\dagger \Phi_2 + (\mu_3 \Phi_1^\dagger \Phi_2 + h.c.) \\ & + \lambda_1 (\Phi_1^\dagger \Phi_1)^2 + \lambda_2 (\Phi_2^\dagger \Phi_2)^2 + \lambda_3 (\Phi_1^\dagger \Phi_1)(\Phi_2^\dagger \Phi_2) \\ & + \lambda_4 (\Phi_1^\dagger \Phi_2)(\Phi_2^\dagger \Phi_1) + (\lambda_5 (\Phi_1^\dagger \Phi_2)^2 + h.c.) \\ & + (\Phi_1^\dagger \Phi_1)(\lambda_6 (\Phi_1^\dagger \Phi_2) + h.c.) \\ & + (\Phi_2^\dagger \Phi_2)(\lambda_7 (\Phi_1^\dagger \Phi_2) + h.c.)\,, \end{aligned} \tag{1}$$

where μ_3, λ_5, λ_6 and λ_7 are complex parameters and the others are real parameters. However, not all parameters are physical since they can be modified by a change of basis following the replacement,

$$\begin{pmatrix} \Phi_1 \\ \Phi_2 \end{pmatrix} \to \begin{pmatrix} \Phi_1' \\ \Phi_2' \end{pmatrix} = U_\Phi \begin{pmatrix} \Phi_1 \\ \Phi_2 \end{pmatrix}, \tag{2}$$

where U_Φ is a unitary matrix of dimension 2×2. In order to achieve an invariant vacuum under $U(1)_{EM}$, the expectation values shall be aligned to,

$$\langle \Phi_1 \rangle = \frac{v_1}{\sqrt{2}} \begin{pmatrix} 0 \\ 1 \end{pmatrix} \quad \text{and} \quad \langle \Phi_2 \rangle = \frac{v_2}{\sqrt{2}} \begin{pmatrix} 0 \\ 1 \end{pmatrix}. \tag{3}$$

Regarding this configuration, it is possible to chose a basis where only one of the doublets has a non-zero vacuum expectation value, *i.e.*,

$$\langle \Phi_1' \rangle = \frac{v}{\sqrt{2}} \begin{pmatrix} 0 \\ 1 \end{pmatrix} \quad \text{and} \quad \langle \Phi_2' \rangle = \begin{pmatrix} 0 \\ 0 \end{pmatrix}, \tag{4}$$

where the rotation angle

$$U_\Phi = \begin{pmatrix} \cos\beta & \sin\beta \\ -\sin\beta & \cos\beta \end{pmatrix}, \tag{5}$$

relates the expectation values v_1 and v_2 with v through $v^2 = v_1^2 + v_2^2$ and the angle of rotation satisfies $\tan\beta = v_2/v_1$.

On the other hand, the existence of the second scalar doublet shall be manifested through its couplings with the matter fields through the Yukawa lagrangian. In this basis, the lagrangian is,

$$\begin{aligned} \mathcal{L}_{\text{Yuk}} = &- \overline{Q}_L \cdot y_d \cdot d_R \Phi_1 - \overline{Q}_L \cdot y_u \cdot u_R \tilde{\Phi}_1 \\ &- \overline{Q}_L \cdot G_d \cdot d_R \Phi_2 - \overline{Q}_L \cdot G_u \cdot u_R \tilde{\Phi}_2 \\ &- \overline{L}_L \cdot y_\ell \cdot \ell_R \Phi_1 - \overline{L}_L \cdot G_\ell \cdot \ell_R \tilde{\Phi}_2 + h.c., \end{aligned} \tag{6}$$

where $[\tilde{\Phi}]_i = \varepsilon_{ij} [\Phi]_j$ with ε_{ij} is the antisymmetric Levi-Civita tensor in two dimensions; y_i are the 3×3 Yukawa matrices, which in the diagonal case have inputs proportional to $\sqrt{2}\, m_f/v$, while the matrices G_i contain free parameters in their entries. The interactions of the extra particles are obtained by replacing,

$$\begin{aligned} \Phi_1 &\equiv \frac{1}{\sqrt{2}} \begin{pmatrix} -\imath\sqrt{2}\, G^+ \\ v + h_1^n + \imath\, G_0 \end{pmatrix}, \\ \Phi_2 &\equiv \frac{1}{\sqrt{2}} \begin{pmatrix} \sqrt{2} H^+ \\ h_2^n + \imath\, h_3^n \end{pmatrix}. \end{aligned} \tag{7}$$

where G_0 and G^+ are the Goldstone bosons that give mass to the particles. The physical mass of the charged scalar boson is,

$$m_{H^+}^2 = \mu_2 + \lambda_3 \frac{v^2}{2}, \tag{8}$$

and the mass matrix for the scalar neutral states is,

$$m_0^2 = \begin{pmatrix} \lambda_1 v^2 & \Re\lambda_6 \frac{v^2}{2} & -\Im\lambda_6 \frac{v^2}{2} \\ \Re\lambda_6 \frac{v^2}{2} & m_{22}^2 & -\Im\lambda_5 \frac{v^2}{2} \\ -\Im\lambda_6 \frac{v^2}{2} & -\Im\lambda_5 \frac{v^2}{2} & m_{33}^2 \end{pmatrix}, \tag{9}$$

with $m_{22}^2 = (1/4)(2m_{H^+}^2 + (\lambda_4 + 2\Re\lambda_5))$ and $m_{33}^2 = (1/4)(2m_{H^+}^2 + (\lambda_4 - 2\Re\lambda_5))$. As for the mass eigenstates, H_i, they are obtained from a unitary rotation,

$$H_i = U_{ij} H_j^n, \tag{10}$$

where $H_i = (h\ H\ A)^T$ and $H^n = (h_1^n\ h_2^n\ h_3^n)$. This model has many phenomenological implications and depending on the theoretical constraints imposed it is possible to reduce the parameter space.

In this paper we will analyze a small set of the parameter space to understand the phenomenological implications of the 2HDM model in comparison to the SM within the LHC and the FCC.

3. Phenomenological analysis

To understand the differences between the theoretical models, it is essential to analyze Monte Carlo simulations that recreate collisions at high energies. In this work, we will use the public code `MadGraph` [27] to dive into the collisions that takes place at the LHC and the FCC.

In this assignment, we focus on the process $pp \to jjh$ with special interest in the kinematical reconstruction of the jets. The Monte Carlo simulations were adjusted in such a way that the events must satisfy the following LHC kinematic cuts at a center of mass energy of $\sqrt{s} = 13$ TeV,

$$\begin{aligned} &p_{T,jet} > 20 \text{ GeV}, \\ &\eta_{T,jet} < 5, \\ &\Delta R_{jj} < 0.4. \end{aligned} \tag{11}$$

Furthermore, for the Parton Distribution Functions, we used NNPDF3.0 [28] which is already implemented in MadGraph 5. Finally, in order to understand the main phenomenological differences between the SM and the 2HDM, al Leading Order (LO), at two different center of mass energies, we study also the FCC enviroment, at $\sqrt{s} = 100$ TeV, with the same kinematical cuts as for the LHC.

In Figs. 1-3, we present the results of the distributions obtained for both models for the LHC configuration. In Fig. 1, the angular distribution of the jet separation is presented. We observe that the 2HDM model presents significant differences that reach the order of 50% with respect to the SM prediction at $\phi \sim 1$.

The transverse momentum distribution of the leading jet is presented in Fig. 2. For low p_T, large deviations of the order of 200% are observed, however, it is possible that Next-to-Leading Order (NLO) corrections decrease this discrepancy. On the other hand, for large p_T we have deviations of 50% which might be originated due to stronger couplings of

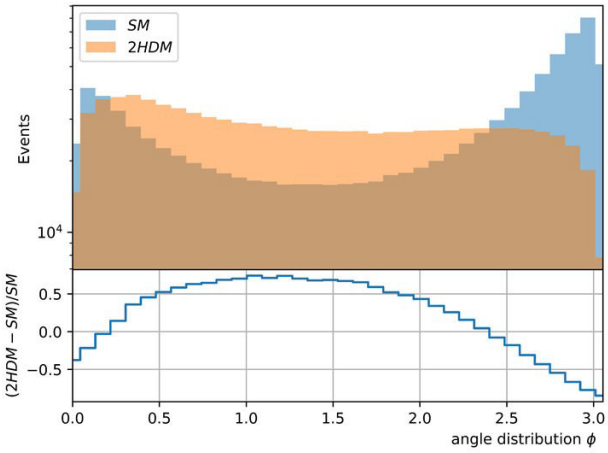

FIGURE 1. Comparison of the angular separation distribution of the jets between the SM and the 2HDM in the process $pp \to jjH$ at $\sqrt{s} = 13$ TeV with the kinematical cuts in Eq. (11).

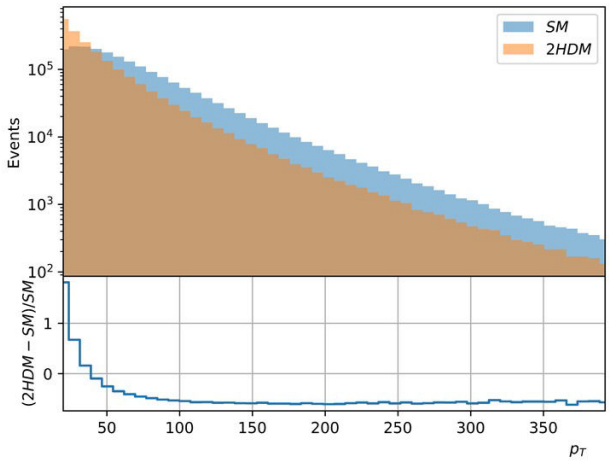

FIGURE 2. Comparison of the transverse momentum of the leading jet between the SM and the 2HDM in the process $pp \to jjH$ at $\sqrt{s} = 13$ TeV with the kinematical cuts in Eq. (11).

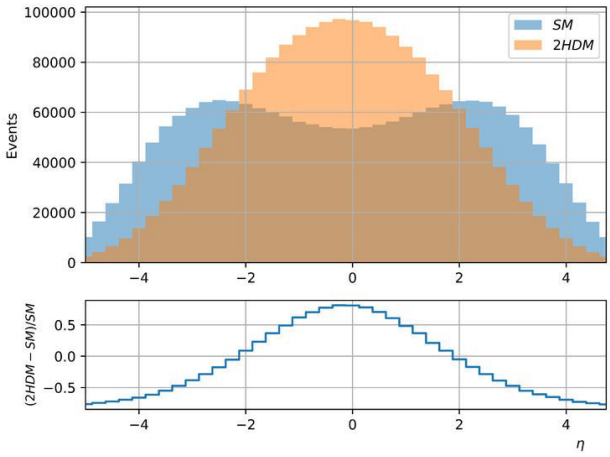

FIGURE 3. Comparison of the rapidity between the SM and the 2HDM in the process $pp \to jjH$ at $\sqrt{s} = 13$ TeV with the kinematical cuts in Eq. (11).

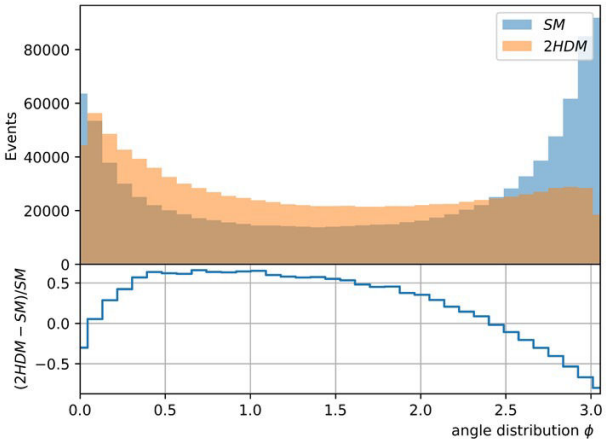

FIGURE 4. Comparison of the angular separation distribution of the jets between the SM and the 2HDM in the process $pp \to jjH$ at $\sqrt{s} = 100$ TeV with the kinematical cuts in Eq. (11).

the new interactions. However, it is possible that these differences might also be reduced with higher order corrections through loop diagrams.

Figure 3 shows the distribution of the rapidity of the jets. We observe that for the SM, the distribution presents a maximum at $\eta \sim \pm 3$, which means that the jets leave the collision in the most forward and backward configuration; however, in the case of the 2HDM most of the events have a distribution centered at zero. Clearly, the percentage comparison will be large, reaching large deviations of the order of 70% at $\eta = 0$.

Similar results for the FCC configuration are presented in Figs. 4-6. In Fig. 4 we find the angular distribution of the jets separation, where we find the largest differences over the whole kinematic range of about $\pm 50\%$ on average.

In Fig. 5 we show the transverse momentum distribution of the leading jet. Again, large deviations are found in the low p_T region, which can possibly be reduced by introducing NLO corrections. For large p_T, deviations of 60% are found.

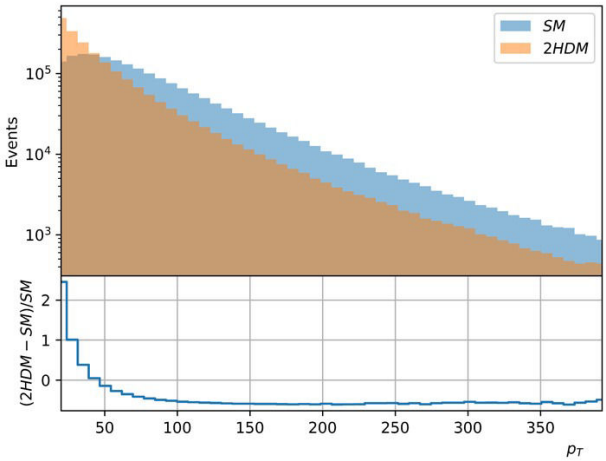

FIGURE 5. Comparison of the transverse momentum of the leading jet between the SM and the 2HDM in the process $pp \to jjH$ at $\sqrt{s} = 100$ TeV with the kinematical cuts in Eq. (11).

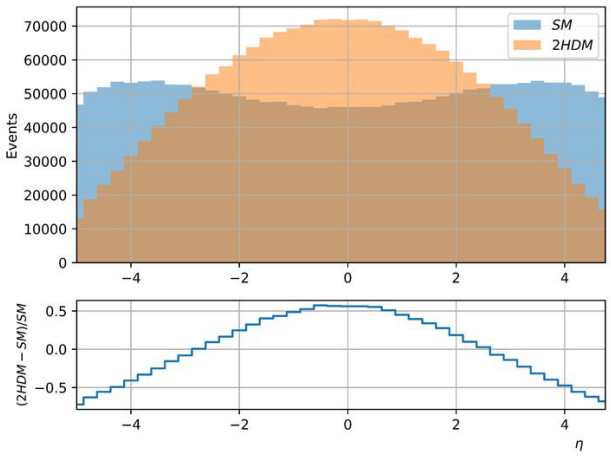

FIGURE 6. Comparison of the rapidity between the SM and the 2HDM in the process $pp \to jjH$ at $\sqrt{s} = 13$ TeV with the kinematical cuts in Eq. (11).

Finally, in Fig. 6 where we observe a behavior similar to that of the LHC for the rapidity of the jets. However, there are noticeable differences between the prediction for the FCC and that for the LHC. In particular, we notice that for the SM, the maximum of the distribution is at $\eta \sim \pm 4$, which implies that the jets in the SM will be produced almost collinear to the beam direction which makes it complicated to measure experimentally. However, for the 2HDM, the jets will be produced mainly in the $\eta = 0$ direction.

4. Conclusions

Experimental evidence supports that there are mild discrepancies between theory and experiment in the context of Standard Model. Hence, in order to solve them, new models that extend its limits seems to be a good approach. One of the best options we currently have to extend the Standard Model is the Two Higgs Doublet Model, as it naturally brings new phenomenology that might fit the subtle results were the Standard Model fail to explain completely. In this work, we study the potential of the 2HDM in the LHC and FCC studies. The phenomenological contributions of the 2HDM make a substantial change to some observables which makes it important enough to be considered for future analyses. In particular, it is important to highlight that higher order corrections can be added in order to reduce the theoretical uncertainties and this shall be a direction to continue this work. A detailed analysis of the phenomenology is under examination for other experimental variables.

Acknowledgments

This research was supported by CONACyT through the Project No. A1- S-33202 (Ciencia Basica), Ciencia de Frontera 2021-2042 and Sistema Nacional de Investigadores. The work is also supported by PROFAPI 2022 Grant No. PRO_A1_024 (Universidad Autónoma de Sinaloa), the COST Action CA16201 (PARTICLEFACE) and MCIN/AEI/10.13039/501100011033, Grant No. PID2020-114473GB-I00.

1. S. Chatrchyan *et al.* [CMS], Observation of a New Boson at a Mass of 125 GeV with the CMS Experiment at the LHC, *Phys. Lett. B* **716** (2012) 30-61, https://doi.org/10.1016/j.physletb.2012.08.021.

2. G. Aad *et al.* [ATLAS], Observation of a new particle in the search for the Standard Model Higgs boson with the ATLAS detector at the LHC, *Phys. Lett. B* **716** (2012) 1-29, https://doi.org/10.1016/j.physletb.2012.08.020.

3. B. Abi *et al.* [Muon g-2], Measurement of the Positive Muon Anomalous Magnetic Moment to 0.46 ppm, *Phys. Rev. Lett.* **126** (2021) 141801, https://doi.org/10.1103/PhysRevLett.126.141801.

4. O. Fischer *et al.* Unveiling Hidden Physics at the LHC, [arXiv:2109.06065 [hep-ph]].

5. S. Weinberg, Phenomenological Lagrangians, *Physica A* **96** (1979) 327-340 https://doi.org/10.1016/0378-4371(79)90223-1.

6. D. de Florian and G. F. R. Sborlini, Hadron plus photon production in polarized hadronic collisions at next-to-leading order accuracy, *Phys. Rev. D* **83** (2011) 074022, https://doi.org/10.1103/PhysRevD.83.074022.

7. D. F. Rentería-Estrada, R. J. Hernández-Pinto and G. F. R. Sborlini, Analysis of the Internal Structure of Hadrons Using Direct Photon Production, *Symmetry* **13** (2021) 942, https://doi.org/10.3390/sym13060942.

8. D. F. Rentería-Estrada, R. J. Hernández-Pinto, G. F. R. Sborlini and P. Zurita, Reconstructing partonic kinematics at colliders with Machine Learning, [arXiv:2112.05043 [hep-ph]].

9. A. Abada *et al.* [FCC], FCC Physics Opportunities: Future Circular Collider Conceptual Design Report Volume 1, *Eur. Phys. J. C* **79** (2019) 474, https://doi.org/10.1140/epjc/s10052-019-6904-3.

10. A. Abada *et al.* [FCC], FCC-ee: The Lepton Collider: Future Circular Collider Conceptual Design Report Volume 2, *Eur. Phys. J. ST* **228** (2019) 261-623, https://doi.org/10.1140/epjst/e2019-900045-4.

11. A. Abada *et al.* [FCC], FCC-hh: The Hadron Collider: Future Circular Collider Conceptual Design Report Volume 3, *Eur. Phys. J. ST* **228** (2019) 755-1107, https://doi.org/10.1140/epjst/e2019-900087-0.

12. A. Abada *et al.* [FCC], HE-LHC: The High-Energy Large Hadron Collider: Future Circular Collider Conceptual Design Report Volume 4, *Eur. Phys. J. ST* **228** (2019)

1109-1382, https://doi.org/10.1140/epjst/e2019-900088-6.

13. A. D. Sakharov, Violation of CP Invariance, C asymmetry, and baryon asymmetry of the universe, *Pisma Zh. Eksp. Teor. Fiz.* **5** (1967) 32-35, https://doi.org/10.1070/PU1991v034n05ABEH002497.

14. S. Vagnozzi, E. Giusarma, O. Mena, K. Freese, M. Gerbino, S. Ho and M. Lattanzi, Unveiling ν secrets with cosmological data: neutrino masses and mass hierarchy, *Phys. Rev. D* **96** (2017) 123503, https://doi.org/10.1103/PhysRevD.96.123503.

15. S. Vagnozzi, S. Dhawan, M. Gerbino, K. Freese, A. Goobar and O. Mena, Constraints on the sum of the neutrino masses in dynamical dark energy models with $w(z) \geq -1$ are tighter than those obtained in ΛCDM, *Phys. Rev. D* **98** (2018) 083501, https://doi.org/10.1103/PhysRevD.98.083501.

16. F. Zwicky, Die Rotverschiebung von extragalaktischen Nebeln, *Helv. Phys. Acta* **6** (1933) 110-127, https://doi.org/10.1007/s10714-008-0707-4.

17. V. C. Rubin and W. K. Ford, Jr., Rotation of the Andromeda Nebula from a Spectroscopic Survey of Emission Regions, *Astrophys. J.* **159** (1970) 379-403, https://doi.org/10.1086/150317.

18. V. C. Rubin, N. Thonnard and W. K. Ford, Jr., Rotational properties of 21 SC galaxies with a large range of luminosities and radii, from NGC 4605 /R = 4kpc/ to UGC 2885 /R = 122 kpc/, *Astrophys. J.* **238** (1980) 471, https://doi.org/10.1086/158003.

19. E. Corbelli and P. Salucci, The Extended Rotation Curve and the Dark Matter Halo of M33, *Mon. Not. Roy. Astron. Soc.* **311** (2000) 441-447, https://doi.org/10.1046/j.1365-8711.2000.03075.x.

20. D. Clowe, M. Bradac, A. H. Gonzalez, M. Markevitch, S. W. Randall, C. Jones and D. Zaritsky, A direct empirical proof of the existence of dark matter, *Astrophys. J. Lett.* **648** (2006) L109-L113, https://doi.org/10.1086/508162.

21. S. W. Allen, A. E. Evrard and A. B. Mantz, Cosmological Parameters from Observations of Galaxy Clusters, *Ann. Rev. Astron. Astrophys.* **49** (2011) 409-470, https://doi.org/10.1146/annurev-astro-081710-102514.

22. P. A. R. Ade *et al.* [Planck], Planck 2015 results. XIII. Cosmological parameters, *Astron. Astrophys.* **594** (2016) A13, https://doi.org/10.1051/0004-6361/201525830.

23. A. G. Riess *et al.* [Supernova Search Team], Observational evidence from supernovae for an accelerating universe and a cosmological constant, *Astron. J.* **116** (1998) 1009-1038, https://doi.org/10.1086/300499.

24. S. Perlmutter *et al.* [Supernova Cosmology Project], Measurements of Ω and Λ from 42 high redshift supernovae, *Astrophys. J.* **517** (1999) 565, https://doi.org/10.1086/307221.

25. H. Georgi, A Model of Soft CP Violation, *Hadronic J.* **1** (1978) 155, HUTP-78/A010.

26. P.A. Zyla *et al.* [Particle Data Group], *Review of Particle Physics* **2020** (2020) 083C01, https://doi.org/10.1093/ptep/ptaa104.

27. J. Alwall, R. Frederix, S. Frixione, V. Hirschi, F. Maltoni, O. Mattelaer, H. S. Shao, T. Stelzer, P. Torrielli and M. Zaro, The automated computation of tree-level and next-to-leading order differential cross sections, and their matching to parton shower simulations, *JHEP* **07** (2014) 079, https://doi.org/10.1007/JHEP07(2014)079.

28. R. D. Ball *et al.* [NNPDF], *JHEP* **04** (2015) 040, https://doi.org/10.1007/JHEP04(2015)040.